Magnetic Field Dependence of Nitrogen−Proton *J* Splittings in ^{15}N-Enriched Human Ubiquitin Resulting from Relaxation Interference and Residual Dipolar Coupling

Nico Tjandra, Stephan Grzesiek, and Ad Bax*

Contribution from the Laboratory of Chemical Physics, National Institutes of Diabetes and Digestive and Kidney Diseases, National Institutes of Health, Bethesda, Maryland 20892-0520

Received January 12, 1996[⊗]

Abstract: One-bond $^1J_{NH}$ couplings have been measured in ^{15}N-enriched human ubiquitin and range from 91.1 to 95.6 Hz. Measurements have been carried out using two different methods and at ^{1}H frequencies of 360, 500, and 600 MHz. The best method yields a precision of *ca* 0.02 Hz, and permits reliable measurement of the small changes (<0.3 Hz) in $^1J_{NH}$ splitting that occur when the magnetic field strength is increased from 8.5 to 14 T. The dependence of the $^1J_{NH}$ splittings on the strength of the static magnetic field originates from two sources: a dynamic frequency shift caused by interference of the ^{15}N chemical shift anisotropy and the ^{15}N−^{1}H dipolar coupling relaxation mechanisms, and a dipolar contribution caused by a small degree of alignment resulting from the anisotropic magnetic susceptibility of the diamagnetic protein. Best fitting of the measured data yields an orientation-independent decrease of 0.11 Hz in the $^1J_{NH}$ splittings at 600 MHz relative to 360 MHz, in perfect agreement with theoretical predictions for the magnitude of the dynamic frequency shift. When fitting the measured *J* values to the theoretical model, containing only the dynamic frequency shift and dipolar coupling contributions, the reduced error in the statistical F-test is smaller than one, assuming a 0.02 Hz rms error in the experimental $^1J_{NH}$ splittings. This confirms that the random error in the measured data J_{NH} values does not exceed 0.02 Hz, and that effects other than the dipolar coupling and dynamic frequency shift are not detectable. Dependence of the change in $^1J_{NH}$ on the orientation of the N−H bond vector within the molecular frame yields experimentally determined axial and rhombic magnetic shielding susceptibility anisotropies of -2.1×10^{-28} and 0.7×10^{-28} cm^3/molecule, respectively. A small improvement of the fit is observed when the amide proton is positioned at a distance above or below the C'_{i-1}−N_i−C^{α}_i plane which is about five times smaller than the out-of-plane distance predicted by *ab initio* calculations on a dipeptide analog in vacuum.

A recent study by Tolman et al.[1] showed that magnetic field alignment of cyanometmyoglobin in aqueous solution, induced by the anisotropic magnetic susceptibility of the protein's paramagnetic metal ion, gives rise to a residual one-bond ^{15}N−^{1}H dipolar coupling. This small residual dipolar coupling is proportional to the square of the static field[2,3] and can be measured from the field dependence of the apparent $^1J_{NH}$ coupling constant, which represents the sum of the dipolar contribution and the true *J* coupling.[1,4] The present study of $^1J_{NH}$ couplings in ubiquitin was initiated to investigate whether the sum of the anisotropic magnetic susceptibility contributions of the backbone peptide bonds and the aromatic side chains would be sufficiently large to observe magnetic alignment of this diamagnetic protein. To this extent, we have carried out highly precise measurements of $^1J_{NH}$ at three different field strengths and using two different measuring techniques. Results indicate that the magnetic field dependence of the $^1J_{NH}$ splittings contains two components: a previously predicted contribution which is independent of orientation and is caused by a dynamic frequency shift,[5] and an orientation-dependent contribution resulting from residual ^{15}N−^{1}H dipolar coupling.

The residual dipolar couplings, which result from incomplete rotational averaging of a protein with an anisotropic magnetic susceptibility tensor, are related to the orientation of the internuclear vector with respect to the magnetic susceptibility tensor and therefore potentially can provide important constraints for determining macromolecular structure. In particular, the ongoing development of NMR spectrometers with stronger magnetic fields makes measurement of this effect increasingly practical. It is therefore important to develop a method which can measure the magnetic field dependence of these dipolar contributions to one-bond *J* couplings as accurately as possible. Here we compare direct measurement of the $^1J_{NH}$ splitting in the ^{15}N dimension of a 2D ^{1}H−^{15}N shift correlation spectrum with values obtained by fitting resonance intensities in a series of $^1J_{NH}$-modulated 2D spectra. It will be shown that the latter approach provides approximately 5-fold higher precision and an estimated error in $^1J_{NH}$ of less than 0.02 Hz. This high precision permits determination of the ubiquitin's magnetic susceptibility tensor and fitting of the data indicates that the N−H bond vector orientations agree well with a planar arrangement of the peptide bond.

Experimental Section

All NMR experiments were carried out at 27 °C on a sample of commercially obtained (U-^{15}N)ubiquitin (VLI Research, Southeastern, PA), 1.4 mM, pH 4.7, 10 mM NaCl. Experiments were carried out on four different Bruker NMR spectrometers, an AMX-360, a DMX-500,

[⊗] Abstract published in *Advance ACS Abstracts,* June 15, 1996.

(1) Tolman, J. R.; Flanagan, J. M.; Kennedy, M. A.; Prestegard, J. H. *Proc. Natl. Acad. Sci. U.S.A.*, **1995**, *92*, 9279−9283.

(2) Bastiaan, E. W.; Maclean, C.; van Zijl, P. C. M.; Bothner-By, A. A. *Annu. Rep. NMR Spectrosc.* **1987**, *19*, 3635−3637.

(3) van Zijl, P. C. M.; MacLean, C.; Bothner-By, A. A. *J. Chem. Phys.* **1985**, *83*, 4410−4417.

(4) Bothner-By, A. A.; Gayathri, C.; van Zijl, P. C. M.; Maclean, C.; Lai, J.-J.; Smith, K. M. *Magn. Reson. Chem.* **1985**, *23*, 935−938. Gayathri, C.; Bothner-By, A. A.; van Zijl, P. C. M.; Maclean, C. *Chem. Phys. Lett.* **1982**, *87*, 192−196.

(5) Werbelow, L. G. *Encyclopedia of Nuclear Magnetic Resonance*; Grant, D. M., Harris, R. K., Editors-in-Chief; Wiley: London, 1996, Vol. 6, pp 4072−4078.

S0002-7863(96)00106-0

an AMX-600, and a DMX-750, operating at ^{1}H resonance frequencies of 360, 500, 600, and 750 MHz, respectively. All spectrometers were equipped with triple resonance (^{1}H, ^{13}C, ^{15}N) pulsed field gradient probeheads.

Two-dimensional ^{1}H−^{15}N HSQC spectra were recorded without ^{1}H decoupling during the ^{15}N evolution period (t_1) using the pulse scheme of Figure 1A. Acquisition times in the t_1 and t_2 dimensions were 100 and 83 ms at all four field strengths and the total measuring time per 2D spectrum was 9 h (360 MHz), 7 h (500, 600 MHz), and 2.3 h (750 MHz). In order to estimate the precision of the measurements, each spectrum was recorded twice. A hardware problem caused field-frequency lock instabilities during the measurements at 750 MHz and resulted in slightly lower reproducibility of the measured $^1J_{NH}$ splittings. Time domain data were apodized with a 60°-shifted squared sine bell (t_2) and a 45°-shifted sine bell (t_1) function and zero-filled prior to 2D Fourier transformation to yield a digital resolution of 4.5 (F_2) and 0.9 Hz (F_1). The signal-to-noise ratio of these spectra was *ca.* 125:1 (360 MHz), 500:1 (500 MHz, 600 MHz), and 350:1 (750 MHz). Spectra were processed using the NMRPipe software package,[6] and peak positions were determined by contour averaging using the program PIPP,[7] as described previously.[8] Resonance assignments were taken from Wang et al.[9]

A series of ten $^1J_{HN}$-modulated 2D ^{1}H−^{15}N HSQC spectra was recorded at 360, 500, and 600 MHz, using the pulse scheme of Figure 1B. Acquisition times in the t_1 and t_2 dimensions were 80 and 83 ms at all three field strengths. Time domain data were apodized with a 60°-shifted squared sine bell (t_2) and a 60°-shifted sine bell (t_1) function and zero-filled prior to 2D Fourier transformation to yield a digital resolution of 4.5 (F_2) and 3.9 Hz (F_1). Dephasing delays, 2Δ, were 45.3, 46.1, 47.5, 48.9, 50.3, 56.5, 57.4, 58.3, 59.9, and 61.0 ms. These delays included the durations of the pulsed field gradients, G4, but not the duration of the ^{15}N 180°$_{\phi_3}$ pulse which must be taken into account when calculating the J splittings (see Results section). The total measuring time for each series of ten experiments was 40 h at 360 MHz and 18 h at 500 and 600 MHz. ^{15}N 90° pulse widths were 21 (360 MHz), 44 (500 MHz), and 46 μs (600 MHz); ^{1}H 90° pulse widths were 8 (360 and 500 MHz) and 10 μs (600 MHz). In order to obtain estimates for the random error in each of the measurements, the series at 360 and 600 MHz were recorded twice.

Results and Discussion

Various different methods for measurement of $^1J_{NH}$ splittings were tested experimentally. Although numerous schemes can be devised for measuring $^1J_{NH}$, achieving an accuracy significantly better than 0.1 Hz requires extreme care in order to minimize all sources of possible artifacts. Even minute imperfections such as a 1° phase distortion, not visible to the eye, can shift the resonance position by a tenth of a hertz. The presence of very weak spurious resonances can have similar effects. Experimentally, we found that the simplest schemes provided the most robust measurement and the results obtained with two such schemes are discussed below.

$^1J_{NH}$-Coupled 2D ^{1}H−^{15}N Correlation. One particularly straightforward method for obtaining $^1J_{NH}$ involves simply measuring the splittings in a 2D ^{1}H−^{15}N correlation spectrum, recorded in the absence of heteronuclear decoupling during either the evolution or the detection period. We prefer to measure the splitting from HSQC spectra decoupled in the F_2 dimension, but with ^{15}N−^{1}H coupling present in the F_1 dimension (Figure 1A). This choice is motivated by the longer transverse relaxation times of ^{15}N relative to ^{1}H^N, resulting in higher resolution in the F_1 dimension. A potential problem with this method can occur if protons with a long-range coupling to ^{15}N are subject to non-first-order ^{1}H−^{1}H J coupling. Although the ^{15}N−^{1}H long-range couplings are typically not resolved in the F_1 dimension of the 2D spectrum, strong ^{1}H−^{1}H coupling involving, for example, one of the ^{1}H$^\beta$ spins coupled to ^{15}N can give rise to a small asymmetry in the line shape of the components of the ^{15}N $^1J_{NH}$ doublet. The degree of non-first-order ^{1}H−^{1}H coupling, and thereby the extent of the line shape asymmetry, varies with the strength of the magnetic field and can result in small perturbations of the measured $^1J_{NH}$ splitting. The substantial degree of resonance overlap in the ^{1}H^N-coupled HSQC spectrum, particularly at lower magnetic field strengths, constitutes another major drawback for this method.

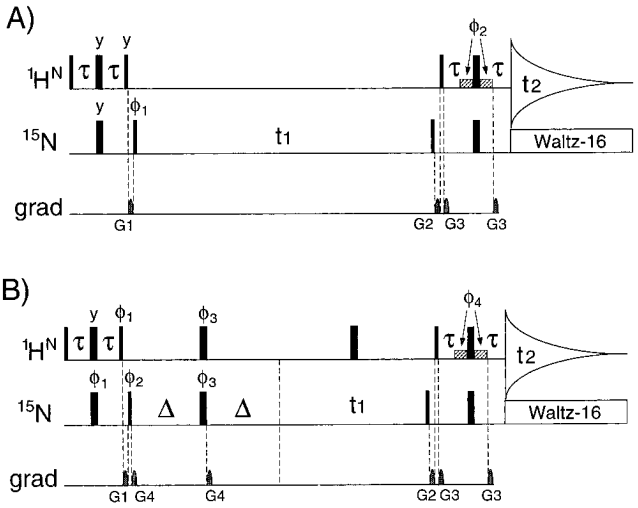

Figure 1. Pulse schemes of (A) ^{1}H-coupled HSQC (heteronuclear single quantum correlation) and (B) $^1J_{NH}$-modulated HSQC. Narrow and wide bars correspond to 90° and 180° flip angles, respectively. Pulses for which the RF phase is not indicated are applied along the x axis. The two low-power pulses (1 ms each) immediately adjacent to the last 180° ^{1}H pulse correspond to 90° flip angles, applied selectively to the H_2O resonance, and are part of the WATERGATE[35] water suppression scheme. For (A), the phase cycling is $\phi_1 = x,-x,-x,x$; $\phi_2 = -x$; receiver = $x,-x-x,x$. Quadrature detection in the t_1 dimension is obtained using the States-TPPI protocol, incrementing ϕ_1. To obtain a perfect F_1 baseline and exact phasing with a 180° linearly frequency-dependent phase correction, the duration of the first t_1 increment is set to (DW$_1$/2 − 4/π × τ_{90}(N)), where DW$_1$ is the t_1 increment.[36] For (B), the phase cycling is $\phi_1 = 8(y),8(-y)$; ϕ_2 $x,-x$; $\phi_3 = 2(x),2(y),2(-x),2(-y)$; $\phi_4 = -x$; receiver = $x,2(-x),2(x),2(-x),x,-x,2(x),2(-x),2(x),-x$. Quadrature detection in the t_1 dimension is obtained using the States-TPPI protocol, simultaneously incrementing ϕ_2 and ϕ_3. Provided the centers of the ^{1}H and ^{15}N 180° pulses, applied at the midpoint of 2Δ, coincide and τ_{180}(H) ≪ τ_{180}(N), a fraction 2/π of τ_{180}(N) needs to be added to the duration of 2Δ when calculating $^1J_{NH}$ from the intensity modulation pattern. For both schemes, pulsed field gradients have a sine-bell shape and an amplitude of 25 G/cm at their center. Gradient durations: $G_{1,2,3,4}$ = 2.5, 1.0, 0.4, 2.3 ms.

A small region of the (F_1-^{1}H^N)-coupled HSQC spectrum of human ubiquitin, recorded at field strengths of 360, 500, 600, and 750 MHz, is shown in Figure 2. The reproducibility of the measured doublet splittings was established by recording each spectrum twice and the averaged $^1J_{NH}$ splittings are reported in supporting information, Table 1, for each of the four magnetic field strengths. The pairwise root-mean-square differences between the two sets of J couplings measured at each field strength were 0.32 (360 MHz), 0.26 (500 MHz), 0.15 (600 MHz), and 0.36 Hz (750 MHz). The pairwise difference between the averaged 360- and 750-MHz data sets from these measurements was 0.33 Hz, suggesting that the precision of the $^1J_{NH}$ splittings measured in this manner is insufficient to establish a reliable field dependence of the apparent $^1J_{NH}$ coupling.

(6) Delaglio, F.; Grzesiek, S.; Vuister, G. W.; Zhu, G.; Pfeifer, J.; Bax, A. *J. Biomol. NMR* **1995**, *6*, 277−293.
(7) Garrett, D. S.; Powers, R.; Gronenborn, A. M.; Clore, G. M. *J. Magn. Reson.* **1991**, *95*, 214−220.
(8) Wang, A. C.; Bax, A. *J. Am. Chem. Soc.* **1996**, *118*, 2483−2494.
(9) Wang, A. C.; Grzesiek, S.; Tschudin, R.; Lodi, P. J.; Bax, A. *J. Biomol. NMR* **1995**, *5*, 376−382.

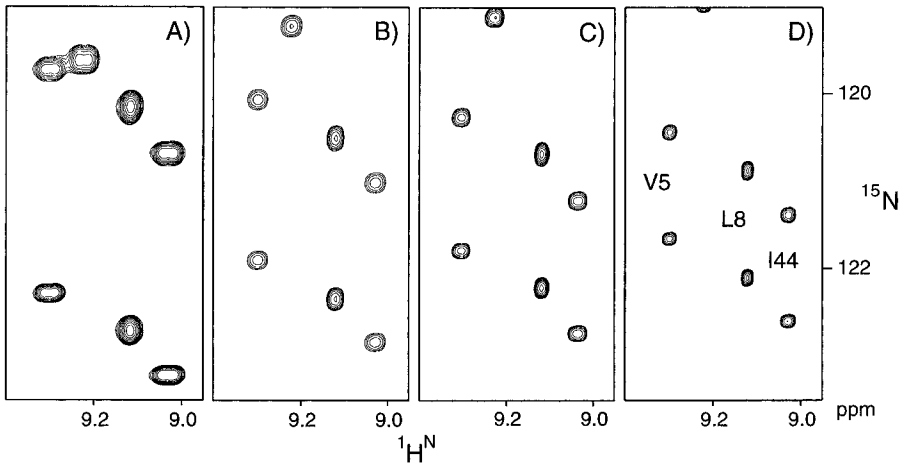

Figure 2. Small sections of the 2D ^{1}H−^{15}N HSQC spectra of human ubiquitin, ^{1}H-coupled in the ^{15}N (F_1) dimension, recorded at (A) 360, (B) 500, (C) 600, and (D) 750 MHz.

$^1J_{NH}$-Modulated 2D HSQC. The second approach tested for accurate measurement of $^1J_{NH}$ involves the introduction of an additional $^1J_{NH}$ evolution period in the regular HSQC pulse scheme (Figure 1B). Although the measurement can be performed as a regular 3D experiment by systematically incrementing the dephasing delay, 2Δ, it is better to record a limited set of 2D spectra, centered around durations of 2Δ, which maximize the dependence of resonance intensity on $^1J_{NH}$. Similar analyses of J modulation patterns previously have been used for measuring $^3J_{H^NH^\alpha}$ and $^1J_{C^\alpha H^\alpha}$.[10−13] In the scheme of Figure 1B, the spin state of the $^1H^N$ during the period where ^{15}N magnetization is transverse is $|\alpha\rangle$ for half the time and $|\beta\rangle$ for the other half. Therefore, the effect of differential relaxation of the ^{15}N doublet components caused by cross correlation between the ^{15}N−^{1}H dipolar and ^{15}N chemical shift anisotropy relaxation mechanisms[14,15] is eliminated. Note that for this reason the standard manner of combining two consecutive 180° ^{1}H pulses into a single 180° pulse[16] can not be used as cross correlation would no longer be eliminated and would affect the measured J modulation frequency.

To a first approximation, the intensity of a 2D ^{1}H−^{15}N correlation in the spectrum recorded with the scheme of Figure 1B is given by

$$I(2\Delta) = C\cos(2\pi J_{NH}\Delta)\exp(-2\Delta/T_2^*) \qquad (1)$$

where T_2* is the inverse of the decay rate of the ^{15}N magnetization as a result of transverse relaxation and unresolved long-range ^{1}H−^{15}N couplings. The absolute value of the derivative of eq 1 with respect to J_{NH} is near a maximum when simultaneously $2\Delta \approx T_2^*$ and $2\Delta \approx (2N + 1)/(2J_{NH})$, with N being an integer number. One-bond J_{NH} values in polypeptides are quite uniform (94 ± 2 Hz), and measured T_2* values were in the 40−80-ms range, substantially shorter than their true T_2 values which fall in the 160−200-ms range.[17] The ten durations of 2Δ used were centered around durations of 47.8 ($N = 4$) and 58.5 ($N = 5$) ms.

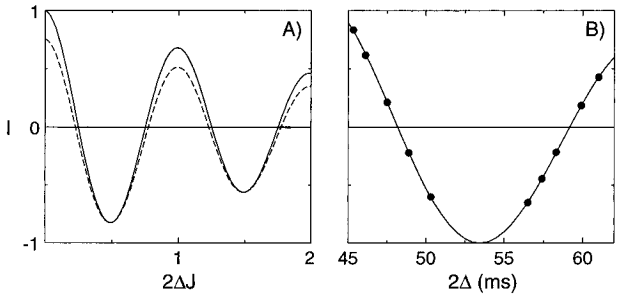

Figure 3. Modulation of resonance intensity, I, as a function of the dephasing delay, 2Δ, with the scheme of Figure 1B. (A) Simulated intensity modulation pattern for cases where the 180° ^{1}H inversion pulse at the midpoint of 2Δ is ideal (solid line) and where this pulse is imperfect and inverts only 90% of the $^1H^N$ magnetization (dashed line). (B) Experimentally observed intensity modulation of the amide of Ile^3, best-fit to eq 2.

Figure 3A compares the J modulation of the intensity of a HSQC correlation spectrum for the case of an ideal 180° ^{1}H inversion at the midpoint of the 2Δ interval with the result anticipated if, due to pulse imperfection, only 90% of the protons are inverted by this pulse. The effect of incomplete inversion by such a pulse[18] cannot be removed by phase cycling or pulsed field gradients[19] and therefore needs to be taken into account in the data analysis. As can be seen from Figure 3A, if the signal were sampled only at time points surrounding a single, odd-numbered zero-crossing, incomplete inversion has the same effect on the position of the zero-crossing as an increase in modulation frequency. At even-numbered zero-crossings, the effect is opposite. As the efficiency of the inversion varies with $^1H^N$ resonance offset and with the different probeheads used at the different magnetic field strengths, this degree of inversion is an unknown variable and the modulation function must be sampled at a minimum of two adjacent zero-crossings, as illustrated in Figure 3B.

Figure 3B shows the best fit between the HSQC intensities, measured with the scheme of Figure 1B for the backbone amide of Ile^3, to the function

$$I(2\Delta) = C[-A + \cos(2\pi^1 J_{NH}\Delta)]\exp(-2\Delta/T_2^*) \qquad (2)$$

(10) Neri, D.; Otting, G.; Wüthrich, K. *J. Am. Chem. Soc.* **1990**, *112*, 3663−3665.
(11) Billeter, M.; Neri, D.; Otting, G.; Qian, Y. Q.; Wüthrich, K. *J. Biomol. NMR* **1992**, *2*, 257−274.
(12) Kuboniwa, H.; Grzesiek, S.; Delaglio, F.; Bax, A. *J. Biomol. NMR* **1994**, *4*, 871−878.
(13) Vuister, G. W.; Delaglio, F.; Bax, A. *J. Biomol. NMR* **1993**, *3*, 67−80.
(14) Gueron, M.; Leroy, J. L.; Griffey, R. H. *J. Am. Chem. Soc.* **1983**, *105*, 7262−7266.
(15) Goldman, M. *J. Magn. Reson.* **1984**, *60*, 437−452.
(16) Kay, L. E.; Ikura, M.; Bax, A. *J. Magn. Reson.* **1991**, *91*, 84−92.
(17) Tjandra, N.; Feller, S. E.; Pastor, R. W.; Bax, A. *J. Am. Chem. Soc.* **1995**, *117*, 12562−12566.
(18) Bodenhausen, G.; Freeman, R.; Turner, D. L. *J. Magn. Reson.* **1977**, *27*, 511−518.
(19) Freeman, R.; Keeler, J. *J. Magn. Reson.* **1981**, *41*, 484−487.

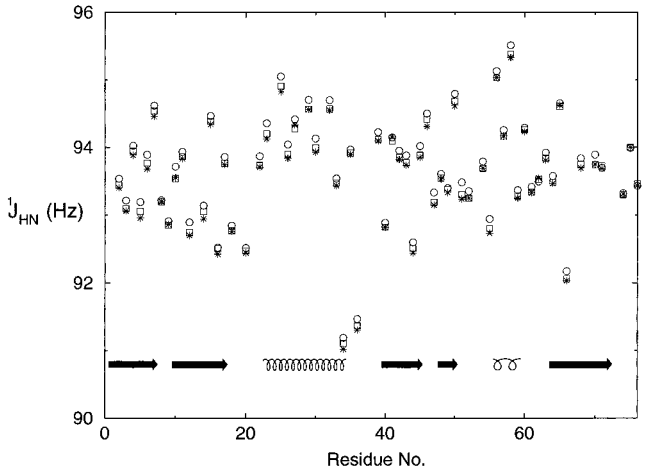

Figure 4. $^1J_{NH}$ splittings measured for the backbone amides of ubiquitin at (○) 360 MHz, (□) 500 MHz, and (*) 600 MHz, using the pulse scheme of Figure 1B. For reference, the polypeptide secondary structure[24] is shown at the bottom of the diagram. $^1J_{NH}$ values at 360 and 600 MHz are the averages obtained from two separate sets of experiments and have a smaller random error than the $^1J_{NH}$ values measured at 500 MHz, which result from a single set of experiments. The secondary structure of the polypeptide is marked solely for the purpose of indicating approximately where in the structure each residue is located, and that $^1J_{NH}$ values in the α-helix (Asn^{25}-Lys^{33}), on average, are larger and more homogeneous than in other regions of the protein.

where A accounts for the unmodulated fraction of the magnetization. The effect of the finite duration of the 180° ^{15}N pulse applied at the midpoint of the dephasing interval, 2Δ, is another detail which needs to be accounted for. Provided the midpoints of the ^{1}H and ^{15}N 180° pulses coincide and the duration of the 180° ^{1}H pulse, τ_{180}(H), is much shorter than that of the 180° ^{15}N pulse, τ_{180}(N), it can be shown that the $^1J_{NH}$ dephasing angle accumulated during the 180° ^{15}N pulse is $4^1J_{NH}\tau_{180}$(N). Thus, a fraction $2/\pi$ of the 180° ^{15}N pulse must be added to the dephasing delay, 2Δ, prior to calculating $^1J_{NH}$.[20]

In principle, the effects of transverse cross relaxation between the two ^{15}N doublet components[15] also must be taken into account as this affects the evolution of the two ^{15}N doublet components during the dephasing period, 2Δ. This cross relaxation is usually neglected for non-overlapping doublet components, and its rate depends on the spectral density function evaluated at the ^{1}H frequency.[15] Numerical simulations of the spin system evolution, carried out for human ubiquitin and assuming isotropic rotational diffusion with a correlation time of 4.1 ns, indicate that this effect results in an increase of the $^1J_{NH}$ coupling by 9×10^{-4} Hz when the field strength is increased from 8.5 to 14 T. This effect is much smaller than the uncertainty in the experimental results and therefore may be ignored.

Measurements of $^1J_{NH}$ with the pulse scheme of Figure 1B and the fitting procedure described above yielded highly reproducible values. The pairwise rmsd between successive measurements of 62 $^1J_{NH}$ values was 0.031 and 0.015 Hz at 360 and 600 MHz, respectively. This indicates that the respective random uncertainties in the $^1J_{NH}$ values, averaged over the two measurements, are only 0.016 and 0.008 Hz. The values are plotted in Figure 4 and are listed in supporting information, Table 1. Measured $^1J_{NH}$ values fall in the 91.1−95.6-Hz range, and the values measured at the three different field strengths are clearly very close to one another, ranging from a 0.06-Hz increase to a 0.24-Hz decrease when the field strength is increased from 8.5 (360 MHz) to 14.1 T (600 MHz).

Dynamic Frequency Shift Contribution to $^1J_{NH}$. Before describing how the magnetic field dependence of the $^1J_{NH}$ splittings can be related to the orientation and magnitude of the magnetic susceptibility tensor, another factor which causes a measurable change in $^1J_{NH}$ with field must be considered first. As is well-known, peptide ^{15}N doublet components relax at very different rates due to interference (cross-correlation) between ^{15}N chemical shift anisotropy and ^{1}H−^{15}N dipolar coupling relaxation mechanisms.[14,15] The ^{15}N chemical shift anisotropy (CSA) tensor tends to be nearly axially symmetric with a magnitude, $\sigma_\perp - \sigma_\parallel$ of ∼160 ppm and an angle, η, of ∼24° between the unique axis of the CSA tensor and the ^{15}N−^{1}H bond vector.[21,22] Thus, the spectral density and thereby its imaginary component, are very different for the two doublet components. The imaginary component of the spectral density gives rise to a small shift in the resonance frequency, often referred to as the dynamic frequency shift, which therefore is different for the two components of the ^{15}N doublet and appears as a change in the $^1J_{NH}$ splitting. For isotropic molecular diffusion, with a rotational correlation time τ_c, the change in the $^1J_{NH}$ splitting resulting from this dynamic frequency shift effect is a function of the strength of the magnetic field, B_o, and is given by[5]

$$\delta_{DFS}(B_o) = S^2(20\pi^3)^{-1}h(\sigma_\parallel - \sigma_\perp)(3\cos^2\eta - 1)\gamma_N\gamma_H(r_{NH})^{-3} \times [1 + (\gamma_N B_o \tau_c)^{-2}]^{-1} = \delta_{DFS}(\infty)[1 + (\gamma_N B_o \tau_c)^{-2}]^{-1} \quad (3)$$

where h is Planck's constant, γ_N and γ_H are the gyromagnetic ratios for ^{15}N and ^{1}H, η is the angle between the unique axes of the dipolar and CSA tensors, and r_{NH} is the N−H internuclear distance, assumed to be 1.02 Å. $\boldsymbol{S}^2$ is the generalized order parameter, describing the effect of fast internal motions,[23] and $\gamma_N B_o = \omega_N$ is the angular ^{15}N Larmor frequency. The magnitude of δ_{DFS} as a function of $\omega_N\tau_c$ is shown in Figure 5, assuming $\boldsymbol{S}^2 = 1$. As can be seen from this figure, in the slow motion limit ($\omega_N\tau_c \gg 1$) δ_{DFS} approaches $\delta_{DFS}(\infty) \approx -0.54$ Hz. In principle, there is also contribution to the $^1J_{NH}$ splitting from cross-correlation between $^1H^N$ CSA and ^{1}H−^{15}N dipolar coupling, but as this contribution is proportional to $[1 + (\omega_H\tau_c)^{-2}]^{-1}$ it may be considered constant over the range of magnetic field strengths used in this study ($\omega_H\tau_c \gg 1$), and it is therefore ignored.

Assuming isotropic rotational diffusion with $\tau_c = 4.1$ ns, $\eta = 24°$, $\sigma_\parallel - \sigma_\perp = 160$ ppm, and a uniform $\boldsymbol{S}^2$ value of 0.85, δ_{DFS} is 0.214, 0.288, and 0.325 Hz at ^{15}N resonance frequencies of 36.5, 50.7, and 60.8 MHz, respectively. A recent ^{15}N NMR relaxation study indicates that rotational diffusion of ubiquitin is not quite isotropic but, to a good approximation, is described by an axially symmetric rotational diffusion tensor, **D**, with $D_\parallel/D_\perp \approx 1.17$, and an apparent rotational correlation time, $\tau_c = 1/(2\ \mathrm{Tr}\ \mathbf{D})$, of 4.1 ns.[17] For non-isotropic but axially symmetric rotational diffusion, $\delta_{DFS}(B_o)$ is described by[5]

(20) Ernst, R. R.; Bodenhausen, G.; Wokaun, A. *Principles of Nuclear Magnetic Resonance in One and Two Dimensions*; Clarendon Press, 1986; p 121.

(21) Oas, T. G.; Hartzell, C. J.; Dahlquist, F. W.; Drobny, G. P. *J. Am. Chem. Soc.* **1987**, *109*, 5962−5966.

(22) Hiyama, Y.; Niu, C.-H.; Silverton, J. V.; Bavoso, A.; Torchia, D. A. *J. Am. Chem. Soc.* **1988**, *110*, 2378−2383.

(23) Lipari, G.; Szabo. A. *J. Am. Chem. Soc.* **1982**, *104*, 4546−4558.

(24) Vijay-Kumar, S.; Bugg, C. E.; Cook, W. J. *J. Mol. Biol.* **1987**, *194*, 531−544.

(25) Brünger, A. T. *X-PLOR Version 3.1: A System for X-ray Crystallography and NMR*; Yale University Press: New Haven, CT, 1992.

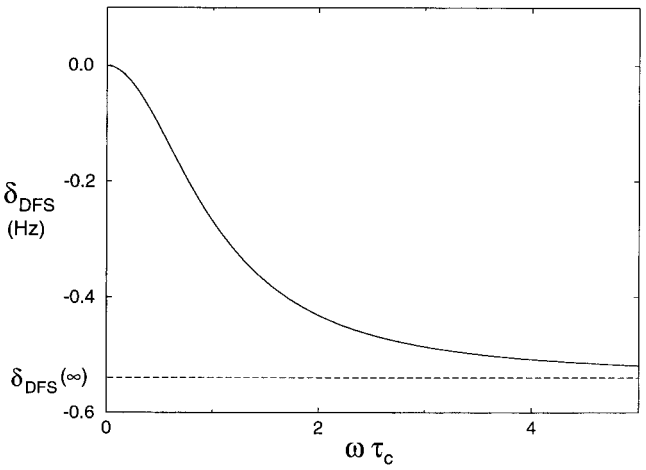

Figure 5. Dependence of the dynamic frequency shift contribution on $\omega_N\tau_c$, assuming $S^2 = 1$, an axially symmetric ^{15}N CSA tensor with $\sigma_\perp - \sigma_\parallel = 160$ ppm, and a 24° angle between the unique axis of the CSA tensor and the N−H bond vector.

$$\delta_{DFS}(B_o) = S^2(40\pi^3)^{-1}h(\sigma_\parallel - \sigma_\perp)\gamma_N\gamma_H(r_{NH})^{-3} \times \{(3\cos^2\eta_D - 1)(3\cos^2\eta_C - 1)/[1 + (\gamma_N B_o\tau_1)^{-2}] + 12\cos\eta_D\cos\eta_C\sin\eta_D\sin\eta_C\cos(\phi_D - \phi_C)/[1 + (\gamma_N B_o\tau_2)^{-2}] + 3\sin^2\eta_D\sin^2\eta_C\cos(2\phi_D - 2\phi_C)/[1 + (\gamma_N B_o\tau_3)^{-2}]\} \quad (4)$$

with $\tau_1 = (6D_\perp)^{-1}$, $\tau_2 = (D_\parallel + 5D_\perp)^{-1}$, and $\tau_3 = (4D_\parallel + 2D_\perp)^{-1}$. The angle between the unique axes of the dipolar and diffusion tensors is η_D, and that between the axially symmetric CSA tensor and the diffusion tensor is η_C. The difference $\phi_D - \phi_C$ refers to the angle between projections of the unique axes of the dipolar and CSA tensors on the plane perpendicular to the unique axis of the diffusion tensor. Residue-specific values of δ_{DFS}, which take into account the previously measured S^2 values and the diffusion anisotropy, have been calculated using eq 4, and these values are reported in supporting information, Table 2.

Dipolar Contribution to $^1J_{NH}$ Splitting. In the principal axis system of the magnetic susceptibility tensor, the $^1H-^{15}N$ dipolar coupling contribution, δ_{dip}, to the $^1J_{NH}$ splitting is given by[1,4]

$$\delta_{dip}(\theta,\phi) = -(B_o^2/15kT)[\gamma_N\gamma_N h/(4\pi^2 r_{HN}^3)] \times [\Delta\chi_a(3\cos^2\theta - 1) + {}^3/_2\Delta\chi_r(\sin^2\theta\cos 2\phi)] \quad (5)$$

where B_o is the applied magnetic field, $\Delta\chi_a$ and $\Delta\chi_r$ are the axial and rhombic components of the magnetic susceptibility tensor ($\Delta\chi_a = \chi_{zz} - (\chi_{xx} + \chi_{yy})/2$; $\Delta\chi_r = \chi_{xx} - \chi_{yy}$), and θ and ϕ are cylindrical coordinates describing the orientation of the N-H bond vector in the principal axis system of the magnetic susceptibility tensor.

Magnetic Susceptibility Anisotropy from $^1J_{NH}$ Splittings. As described above, the B_o-dependent $^1J_{NH}$ splitting is the sum of three components:

$$^1J_{NH}(B_o) = {}^1J_{NH}(0) + \delta_{dip}(\theta,\phi) + \delta_{DFS}(B_o) \quad (6)$$

where $^1J_{NH}(0)$ is the true $^1J_{NH}$ scalar coupling, and $\delta_{dip}(\theta,\phi)$ and $\delta_{DFS}(B_o)$ are the contributions from the dipolar coupling and the dynamic frequency shift described above. For 59 residues in ubiquitin with order parameters greater than 0.7, values for $^1J_{NH}(B_o)$ have been measured at three different fields, and therefore these values can be used to determine $\Delta\chi_a$, $\Delta\chi_r$, and the three variables describing the orientation of the susceptibility tensor in the molecular frame. A prerequisite for such a fitting procedure is that the orientations of the N−H bond vectors in the molecular frame are known. In our calculations the orientations of these vectors are obtained from the ubiquitin X-ray structure coordinates,[24] using the program X-PLOR[25] to determine the positions of the amide protons, assuming planar peptide bond geometry. Ignoring differences in S^2 values for the different amides, and assuming isotropic rotational diffusion, $\delta_{DFS}(\infty)$ can also be determined from such a fitting procedure. Alternatively, residue-specific values of $\delta_{DFS}(B_o)$ can be taken from supporting information, Table 2, which have been calculated using the order parameters and axially symmetric rotational diffusion tensor reported previously.[17] Results of both procedures are presented below.

Only data recorded at 360 and 600 MHz were used in the fitting procedures described below as these are the most useful for determining the susceptibility anisotropy. However, as can be seen from Figure 4, the splittings recorded at 500 MHz confirm that $^1J_{NH}$ changes monotonically with field. The 500-MHz data have not been recorded twice and the uncertainty in the measured values is therefore unknown and presumably at least a factor $2^{1/2}$ higher than that for the data recorded at 600 MHz. The values of $\Delta\chi_a$, $\Delta\chi_r$, and the three Euler angles θ', ϕ', and ψ describing the orientation of the susceptibility tensor in the coordinate frame of the ubiquitin X-ray structure are those which minimize the difference, E, between the observed ("obs") and predicted ("pred") change in $^1J_{NH}$ splitting with field:

$$E = \sum_N[(J_{600}^{obs} - J_{360}^{obs}) - (J_{600}^{pred} - J_{360}^{pred})]^2/2q^2 \quad (7)$$

where q is the estimated random error (0.02 Hz) in the observed $^1J_{NH}$ splittings at 600- and 360-MHz ^1H frequency, and the summation extends over all N residues ($N = 59$) with $S^2 \geq 0.7$ for which $^1J_{NH}$ could be measured at both field strengths. E is a six-dimensional function and is minimized by means of a Powell optimization procedure. Substitution of the magnetic anisotropy susceptibility parameters and a dynamic frequency shift contribution, obtained in this manner, into eqs 5 and 6 yields a predicted difference between $^1J_{NH}$ values measured at 360 and 600 MHz. Table 1 lists the results of fitting the measured data to six different models: (I) δ_{DFS}, $\Delta\chi_a$, and $\Delta\chi_r$ are all set to zero, (II) $\Delta\chi_a$ and $\Delta\chi_r$ are set to zero but $\delta_{DFS}(\infty)$ is allowed to vary, (III) $\delta_{DFS}(\infty)$ is zero but $\Delta\chi_a$ and $\Delta\chi_r$ are allowed to vary, (IV) δ_{DFS} and $\Delta\chi_a$ are allowed to vary but $\Delta\chi_r = 0$, (V) δ_{DFS}, $\Delta\chi_a$, and $\Delta\chi_r$ are all allowed to vary, and (VI) $\Delta\chi_a$ and $\Delta\chi_r$ are allowed to vary, but residue-specific δ_{DFS} values are calculated using the previously determined diffusion tensor and order parameters.[17] The goodness of the fit to each of these models is reflected in the reduced error function, $E_\nu = E/(N - m)$, where N is the number of independently measured variables, and m is the number of variables used in the fitting procedure. As it is the difference in $^1J_{NH}$ coupling, measured at 600 and 360 MHz, which is fit to the theoretical model, N is the number of residues used in the fit. The results shown in Table 1 indicate that the data are best described by using a non-symmetric magnetic susceptibility tensor, corresponding to five independent variables, and using values for the dynamic frequency shift contribution calculated individually for each residue using eq 4 (model VI). The fit to an axially symmetric susceptibility tensor (model IV) results in a reduced error function which is higher than that for the model using an asymmetric tensor (model V). As is discussed in more detail below, the reduction in E_ν is substantial, indicating that the rhombic component of the susceptibility tensor is significant. Model V assumes that the dynamic frequency shift contribution to the change in $^1J_{NH}$ is the same for all residues considered, whereas eqs 3 and 4

Table 1. Experimental and Calculated Magnetic Susceptibility Parameters for Human Ubiquitin[a]

				$\Delta\chi$, 10^{-28} cm^3/molecule				
model	θ',[b] deg	ϕ',[b] deg	ψ,[b] deg	$\Delta\chi_a$	$\Delta\chi_r$	$\Delta\delta_{DFS}$,[c] 10^{-3} Hz	E_v[d]	m[e]
I[f]				0	0	0	12.69	0
II[g]				0	0	-129 ± 3	2.49	1
III[h]	35 ± 4[m]	103 ± 5	-54 ± 6	-3.6 ± 0.5	1.6 ± 0.3	0	6.89	5
IV[i]	54 ± 6	121 ± 2		-2.3 ± 0.2		-116 ± 5	1.26	4
V[j]	54 ± 4	123 ± 2	-81 ± 5	-2.1 ± 0.2	0.9 ± 0.2	-110 ± 3	1.01	6
VI[k]	57 ± 4	124 ± 2	-83 ± 6	-2.1 ± 0.2	0.7 ± 0.2		0.97	5
X-ray[l]	63	126	-47	-2.36	0.16	-113[n]		

[a] At 27 °C, for all 59 residues ($N = 59$) with non-overlapping ^{15}N−^{1}H correlations and $\boldsymbol{S}^2 \geq 0.7$. [b] Euler angles in the frame of the Brookhaven Protein Data Bank coordinates of ubiquitin.[21] [c] Difference in the dynamic frequency shift contribution to $^1J_{NH}$ at 600 *vs* 360 MHz. [d] Assuming a random error of 0.02 Hz in the measurement of $^1J_{NH}$. [e] Number of variables in the fit. [f] No field dependence of $^1J_{NH}$. [g] Field dependence of $^1J_{NH}$ is caused exclusively by a uniform dynamic frequency shift. [h] Field dependence of $^1J_{NH}$ is caused exclusively by magnetic susceptibility anisotropy. [i] Field dependence of $^1J_{NH}$ results from an axially symmetric susceptibility tensor and a uniform dynamic frequency shift. [j] As model IV, but using an asymmetric susceptibility tensor. [k] As model V, but using dynamic frequency shift contributions (supporting information, Table 3) calculated from previously reported rotational diffusion and order parameters.[17] [l] Susceptibility tensor predicted from the sum of the aromatic ring and peptide bond contributions using X-ray coordinates. [m] Uncertainties correspond to the rms distribution of parameters obtained when repeating the fitting procedure 20 times, each time randomly omitting 20% of the residues. [n] Assuming $\boldsymbol{S}^2 = 0.85$, isotropic rotational diffusion with $\tau_c = 4.1$ ns, and $\eta = 24°$.

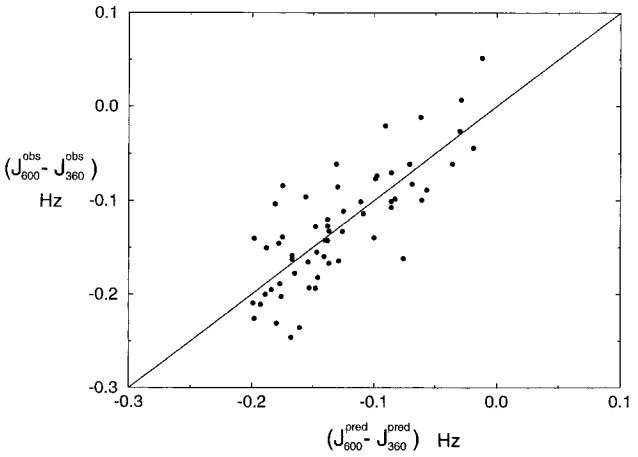

Figure 6. Correlation between measured and calculated difference in $^1J_{NH}$ splitting at 360- and 600-MHz ^{1}H frequency. The calculated difference includes a uniform 0.110-Hz contribution from the dynamic frequency shift, and a dipolar contribution calculated using $\Delta\chi_a = -2.1 \times 10^{-28}$ cm^3, $\Delta\chi_r = 0.9 \times 10^{-28}$ cm^3, $\theta' = 54°$, $\phi' = 123°$, and $\psi = -81°$. The solid line represents the least-squares fit. The correlation coefficient, r, equals 0.79, and the probability that the correlation occurs by chance is smaller than 10^{-6}.

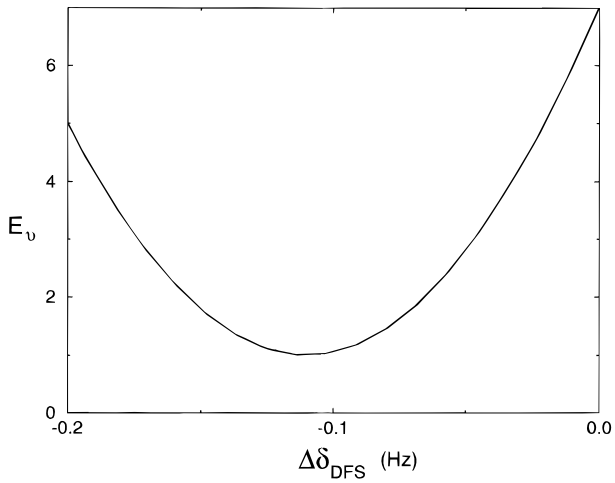

Figure 7. Plot of the reduced error function E_ν as a function of $\Delta\delta_{DFS} = \delta_{DFS}(600\text{ MHz}) - \delta_{DFS}(360\text{ MHz})$, while allowing $\Delta\chi_a$, $\Delta\chi_r$, and the orientation of the susceptibility tensor to vary.

indicate a dependence on the individual order parameter, $\boldsymbol{S}^2$, and the orientation of the N−H bond vector within the axially symmetric diffusion tensor. It is interesting to note that when these effects are taken into account by *calculating* the expected DFS contribution to the change in $^1J_{NH}$ splitting for the individual amides, this results in a better fit to the experimental data (model VI), despite the smaller number of variable parameters used in the fitting procedure. This provides independent validation for the previously derived rotational diffusion parameters.[17]

Figure 6 shows the agreement between the observed differences in $^1J_{NH}$ splitting and values predicted using model V, assuming a uniform difference in dynamic frequency shift contribution to $^1J_{NH}$ of −0.11 Hz at 600 and 360 MHz. The predicted changes in the dipolar contribution to $^1J_{NH}$ range from −0.09 Hz (Thr[55]) to +0.10 Hz (Gln[62]).

Figure 7 shows a plot of E_ν as a function of $\Delta\delta_{DFS} = \delta_{DFS}$(600 MHz) − δ_{DFS}(360 MHz), allowing $\Delta\chi_a$, $\Delta\chi_r$, and the orientation of the susceptibility tensor to vary. This plot shows that the magnitude of the dynamic frequency shift is quite well defined by the NMR data. Randomly deleting 20% of the residues and repeating the fitting procedure confirms that the rms uncertainty in $\Delta\delta_{DFS}$ is only ±0.003 Hz. This random deletion procedure indicates that the susceptibility anisotropy parameters are also well determined.

Statistical Significance. The r-factor of the correlation shown in Figure 6 equals 0.79, and the probability that this correlation occurs by chance, P, is statistically excluded ($P < 10^{-6}$). However, as was pointed out when evaluating the statistical significance of the anisotropy of the ubiquitin rotational diffusion tensor,[17] the N−H bond vectors in ubiquitin are not uniformly distributed and special care must be exercised when using standard protocols for evaluating the significance of the observations. Therefore, two different approaches were followed. First, the statistical F test[26] was used and second, in order to exclude the effect of correlations between the input data, a method based on random permutations was used.

If two fitting procedures with m and $m+n$ variable parameters are performed, then the ratio of their E_ν will follow an F distribution. In particular, a test for the validity of adding n additional terms can be carried out by calculating the following ratio:

$$F = [E(m) - E(m+n)]/[nE_\upsilon(m+n)] \qquad (8)$$

where $E(m)$ is the result of fitting the data using $(N - m)$ degrees

(26) Bevington, P. R.; Robinson, D. K. *Data Reduction and Error Analysis for the Physical Sciences*, 2nd ed.; McGraw-Hill; New York, 1992; pp 205−209.

Table 2. Best Fits of Magnetic Susceptibility Tensor and Uniform Dynamic Frequency Shift to Experimental and Randomly Assigned Data[a]

				$\Delta\chi$, 10^{-28} cm^3/molecule					
	θ',[b] deg	ϕ',[b] deg	ψ,[b] deg	$\Delta\chi_a$	$\Delta\chi_r$	$\Delta\delta_{DFS}$, Hz	E_v	F	$P(F,5,53)$[c]
exp[a]	54	123	−81	−2.09	0.90	−0.110	1.01	15.6	2×10^{-9}
I[a]	−111	50	−39	−1.40	0.81	−0.127	2.30	1.95	0.10
II[a]	−9	23	−6	−1.22	0.36	−0.126	2.33	1.83	0.12
III[a]	−107	71	−75	−1.14	0.21	−0.132	2.36	1.65	0.16
IV[a]	54	164	−63	−1.18	0.12	−0.128	2.37	1.59	0.18

[a] Results listed are for the experimentally assigned amides (exp), and for four data sets (I−IV) where the amide assignments are randomly permuted. Data sets I−IV yield the lowest E_v out of a total of 20 such data sets. [b] Euler angles describing the orientation of the magnetic susceptibility tensor in the frame of the X-ray coordinates. [c] F and $P(F,5,53)$ are calculated relative to the one-parameter model (model II of Table 1) where only the dynamic frequency shift contribution is varied ($E_v = 2.49$).

Table 3. Best Fits of Asymmetric Susceptibility Tensor to Crystallographic and Artificially Perturbed Data[a]

				$\Delta\chi$, 10^{-28} cm^3/molecule					
dataset	θ', deg	ϕ', deg	ψ, deg	$\Delta\chi_a$	$\Delta\chi_r$	δ_{DFS}	E_v	F[b]	$P(F;2,53)$[b]
X-ray[a]	54	123	−81	−2.09	0.90	−0.110	1.01	7.57	1.3×10^{-3}
I[a]	63	120	−37	−2.49	−0.26	−0.110	1.09	5.14	0.009
II[a]	48	122	−86	−2.35	−0.65	−0.113	1.10	4.82	0.012
III[a]	43	127	−17	−2.43	−0.37	−0.111	1.12	4.20	0.020
IV[a]	58	124	0	−2.40	0.53	−0.108	1.13	3.90	0.026

[a] Results listed are calculated using N−H orientations obtained from the crystal structure (X-ray), and four data sets (I−IV) where a random angle was added to the orientation of each N−H bond vector in the plane perpendicular to the z-axis ($\theta,\phi = 54°,123°$) of the susceptibility tensor. Datasets I−IV yield the lowest E_v out of a total of 20 such data sets. [b] F and $P(F;2,53)$ values are calculated relative to the axially symmetric model ($E_v = 1.26$).

of freedom. A large F value justifies the inclusion of the additional terms in the fit. A more convenient measure is the normalized integral of the probability density distribution, $P(F;n,N-m-n)$, which represents the probability that the observed improvement in the $(m + n)$-parameter fit over the m-parameter fit is obtained by chance and P values smaller than 0.01 usually are considered statistically significant.

First we will consider whether the decrease in E_v observed when fitting the data using an axially symmetric susceptibility tensor and $\delta_{DFS}(\infty)$ (corresponding to a total of four independent variables: $\Delta\chi_a$, θ', ϕ', and $\delta_{DFS}(\infty)$) yields a statistically significant improvement over a fit where only $\delta_{DFS}(\infty)$ is allowed to vary (models IV and II in Table 1). The additional three degrees of freedom result in $F = 19.9$ and $P(F;3,55) = 7.5 \times 10^{-9}$. Fitting the data with an asymmetric susceptibility tensor adds two more variables, $\Delta\chi_a$ and ϕ, and yields $F = 7.57$ and $P(F;2,53) = 1.3 \times 10^{-3}$. Thus, the F test indicates that the deviation from axial symmetry of the magnetic susceptibility tensor is statistically significant.

As the distribution of N−H vector orientations in ubiquitin is non-random (for example, the N−H vectors in the Glu[24]-Glu[34] α-helix are nearly parallel to one another) a second test for verifying the statistical significance of the derived susceptibility anisotropy was also carried out: each pair of measured $^1J_{NH}$ values was randomly assigned to one of the 59 residues, thereby removing the correlation between the orientation of the N−H bond vector and the measured difference in J_{NH} splitting. The error function calculation was repeated for 20 different sets of random assignments and the results of the four randomizations which yielded the lowest error function are listed in Table 2. As expected, the fitting of the randomized data sets using model IV does not yield a statistically significant improvement in E_v over the fit using only $\delta_{DFS}(\infty)$ (model II). Finally, the statistical significance of the rhombic component of the susceptibility anisotropy tensor was verified in a similar manner: A random fraction of 360° was added to the orientation of the N−H vector in the plane orthogonal to the unique axis of the axially symmetric susceptibility tensor. Again, the procedure was repeated 20 times and the data were fit using the full six-variable function. The results of the four calculations with the lowest error function are listed in Table 3. In all cases, the reduced error function remains higher compared to the value obtained when using the true N−H bond vector orientations, confirming that the rhombic component indeed is statistically significant.

Agreement with Predicted Magnetic Susceptibility Tensor. For a diamagnetic protein such as ubiquitin, the main contributors to the overall magnetic susceptibility anisotropy are the backbone peptide bonds and the side chains of aromatic residues. To a reasonable approximation, the magnetic anisotropy of the peptide group is axially symmetric and is oriented perpendicular to the peptide plane with a magnitude, $\Delta\chi_a$, of -0.14×10^{-28} cm^3.[27,28] The magnetic anisotropies of the aromatic side chains also are axially symmetric, oriented perpendicular to the plane of the ring, and have $\Delta\chi_a$ values of -1.0×10^{-28} (Phe), -0.94×10^{-28} (Tyr) and -0.53×10^{-28} cm^3 (His).[29] Using the X-ray structure orientations of these groups,[24] the susceptibility tensor is calculated by summing these contributions. This yields a tensor which is nearly axially symmetric (Table 1) and has a magnitude ($\Delta\chi_a = -2.36 \times 10^{-28}$ cm^3) which is in excellent agreement with the experimentally derived values, particularly considering that there is a relatively large uncertainty in the values for $\Delta\chi_a$ of aromatic residues reported in the literature.[28,30,31] The orientation of the symmetry axis is also very similar to that found using the axially symmetric fitting model and deviates by less than 10°. The calculations result in a very small rhombic component ($\Delta\chi_r = 0.16 \times 10^{-28}$ cm^3) which has the same sign and approximately the same orientation as the experimentally observed one. The difference between the predicted and measured rhombic component is 0.6×10^{-28} cm^3, which is smaller than the contribution from a single aromatic

(27) Tigelaar, H. L.; Flygare, W. H. *J. Am. Chem. Soc.* **1972**, *94*, 343−346.
(28) Williamson, M. P.; Asakura, T. *J. Magn. Reson. Ser. B* **1993**, *101*, 63−71.
(29) Giessner-Prettre, C.; Pullman, B. *Q. Rev. Biophys.* **1987**, *20*, 113−172.
(30) Ösapay, K.; Case, D. A. *J. Am. Chem. Soc.* **1991**, *113*, 9436−9444.
(31) Case, D. A. *J. Biomol. NMR* **1995**, *6*, 341−346.

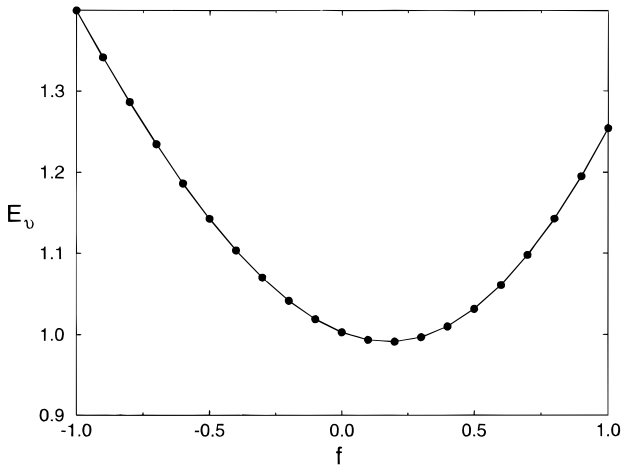

Figure 8. Reduced error function, E_ν, of the fit between $^1J_{NH}$(600 MHz) − $^1J_{NH}$(360 MHz) and model V of Table 1, as a function of the out-of-plane position of the amide proton. The out-of-plane angle predicted by Head-Gordon et al.[29] is scaled by a factor *f*.

ring but outside of the experimental uncertainty of $\pm 0.2 \times 10^{-28}$ cm^3 (Table 1), and possibly could be caused by small differences in the orientations of the aromatic rings in solution relative to the X-ray structure.

Planarity of the Peptide Bond. In the above calculations, the amide protons were positioned in the ubiquitin X-ray structure using the program X-PLOR, which for ubiquitin places these protons very close to the plane defined by C'_{i-1}, N_i, and C^α_i. *Ab initio* calculations by Head-Gordon et al.[32] suggest, however, that H^N is positioned away from the plane by substantially larger amounts which depend on the ϕ and ψ angles of residue *i*. Using the contour diagrams of Figure 9 in ref 32, derived for an alanine dipeptide analog, the amide protons in ubiquitin are rotated out of the plane spanned by C'_{i-1}, N_i, and C^α_i by as much as 25° (supporting information, Table 4, of ref 8). Therefore, when the *ab initio* instead of the X-PLOR positions are used for H^N, the N−H bond vector orientations are significantly different. Fitting the ^{15}N−^{1}H dipolar couplings to the new N−H bond vector orientations results in a considerably poorer fit. However, if the calculated out-of-plane angle is scaled by one-fifth, a small improvement in the fit is observed (Figure 8). Thus, it appears that the *ab initio* calculation qualitatively moves the amide proton out of the peptide plane in the right direction, but overestimates the magnitude of the out-of-plane angle, a result confirmed by a recent study of ^3J couplings involving the amide proton.[8] It is conceivable that the difference between the calculations and experimental results is related to the fact that in proteins nearly all peptide carbonyls and amides form hydrogen bonds, either intramolecular or to the solvent, whereas the *ab initio* calculations were carried out for a dipeptide analog in vacuum. The absence of hydrogen bonding in the dipeptide analog is expected to influence the partial double bond character of the peptide linkage.

Structural Information from Dipolar Coupling. As pointed out by Tolman et al.,[1] the residual dipolar ^{15}N−^{1}H contribution to the $^1J_{NH}$ splitting can be used to derive structural conclusions, provided information regarding the magnitude and orientation of the susceptibility tensor is available. If it is known that the susceptibility tensor is axially symmetric, a reasonable approximation for the magnitude of $\Delta\chi_a$ can be obtained from eq 5 by assuming that the residues which show the largest change in $^1J_{NH}$ splitting (after removing the contribution from the dynamic frequency shift) correspond to θ angles of near 0° and 90°. Assuming that the amides are oriented randomly, the sign of $\Delta\chi_a$ can also be established: if, after removing the DFS contribution, the majority of amides show a decrease in $|^1J_{NH}|$ with increasing field and a smaller fraction shows increases of larger magnitude, $\Delta\chi_a < 0$.

The magnitude of the residual dipolar couplings therefore can be used to constrain the orientation of the N−H vectors relative to the symmetry axis of the susceptibility tensor. However, there remains a 2-fold ambiguity due to the symmetry about $\theta = 90°$ of the $(3\cos^2\theta - 1)$ term in eq 5. Nevertheless, the residual dipolar couplings potentially present a very useful source of structural information which can be used in the later stages of structure determination from NMR data, once the orientation of the susceptibility tensor can be established from a preliminary structure in the manner described above for ubiquitin. In cases where, in addition to ^{15}N−^{1}H dipolar couplings a sufficient number of complementary data can also be obtained for ^{13}C−^{1}H pairs of the polypeptide backbone and side chains, it is not inconceivable that these data can be used as the primary source of information for determining the protein structure in a manner analogous to that proposed for the analysis of solid-state NMR data.[33] In cases where the magnetic susceptibility tensor is not axially symmetric and an approximate structure is known, the dipolar couplings may serve as additional constraints during structure refinement.

As demonstrated in this paper, the dipolar contribution to one-bond *J* splittings in favorable cases can be measured with a precision of a few hundredths of a hertz. The dipolar contributions have been derived from the difference between $^1J_{NH}$ couplings measured at 360- and 600-MHz ^{1}H frequency. If data were measured at 750 or 800 MHz instead of 600 MHz, this would increase the difference in $^1J_{NH}$ splitting, and thereby the accuracy of the dipolar contribution, by 88 and 122%, respectively. Moreover, for many diamagnetic proteins the calculated susceptibility anisotropy is substantially larger than that for ubiquitin, thus reducing the relative uncertainty in the experimentally determined dipolar couplings. For proteins containing one or more paramagnetic sites, the susceptibility anisotropy can be larger by more than an order of magnitude. In such cases where the relative uncertainty in the measured dipolar contributions is small, the main limitation in using this dipolar coupling as a tight constraint in structure calculations is caused by angular fluctuations of the internuclear bond vector. They reduce the dipolar coupling by a factor $\boldsymbol{S}$, where $\boldsymbol{S}$ is the generalized order parameter of the internuclear bond vector (the square root of the number $\boldsymbol{S}^2$ commonly used in relaxation studies).[23] The absolute change in the dipolar coupling as a result of these internal motions is proportional to $\langle 3\cos^2\theta - 1\rangle$ and therefore is minimal when $\theta = 54.7°$. The effect of random measurement error is minimal when the absolute value of the derivative of $\langle 3\cos^2\theta - 1\rangle$ is largest, i.e., for $\theta = 45°$. Thus, for an axially symmetric magnetic susceptibility tensor, the dipolar coupling constraints are most reliable for amides oriented at angles in the 30−60° range relative to the unique axis of the susceptibility tensor.

Concluding Remarks

Our study demonstrates that $^1J_{NH}$ splittings in small proteins can be measured with an accuracy of a few hundredths of a hertz. This permits measurement of the small field-dependent dipolar contributions to $^1J_{NH}$ splittings in ^{15}N-enriched proteins, even in diamagnetic proteins and using a magnetic field of only 14.1 T (600 MHz). The data obtained for ubiquitin uniquely

(32) Head-Gordon, T.; Head-Gordon, M.; Frisch, M. J.; Brooks, C. L., III; Pople, J. A. *J. Am. Chem. Soc.* **1991**, *113*, 5989−5997.

(33) Cross, T. A.; Opella, S. J. *Curr. Opin. Struct. Biol.* **1994**, *4*, 574−581.

define an asymmetric magnetic anisotropy tensor with $\Delta\chi_a = -2.1 \times 10^{-28}$ and $\Delta\chi_r = 0.7 \times 10^{-28}$ cm^3/molecule, in good agreement with values calculated on the basis of contributions from the side chains of the aromatic residues and the peptide bonds, using the ubiquitin X-ray structure.

Fitting of the measured field dependence of $^1J_{NH}$ splittings unambiguously identifies a dynamic frequency shift contribution resulting from a cross-correlation effect between the $^{15}N-^1H$ dipolar coupling and the ^{15}N chemical shift anisotropy tensor. Although such a dynamic frequency shift contribution to *J* couplings has been predicted,[5] to the best of our knowledge this study represents the first experimental observation of such an effect. Compared to a fitting procedure where the dynamic frequency contribution is a variable parameter but the same for each amide, a better fit to the experimental data is obtained when the dynamic frequency shift contribution is calculated separately for each residue, using previously measured anisotropic rotational diffusion and order parameters. This provides independent confirmation for the validity of these motional parameters.

When fitting the measured *J* values to the theoretical model, containing only the dynamic frequency shift and dipolar coupling contributions, the reduced error in the statistical *F*-test is smaller than one, assuming a 0.02 Hz rms error in the experimental $^1J_{NH}$ splittings. This confirms that the random error in the measured data J_{NH} values must be smaller than 0.02 Hz. It also indicates that other effects which are expected to change the $^1J_{NH}$ splitting as a function of field strength, such as the Fermi contact term contribution to the $^1J_{NH}$ coupling and the fact that the $^1J_{NH}$ coupling itself is a tensorial and not a scalar property, must be considerably smaller than 0.02 Hz.

Residual $^{13}C-^1H$ dipolar couplings are approximately 2-fold larger than $^{15}N-^1H$ couplings and potentially also provide useful structural constraints although the precision of the measurement is adversely affected by the short transverse relaxation time of ^{13}C relative to ^{15}N. Nevertheless, it is anticipated that combined use of $^{15}N-^1H$ and $^{13}C-^1H$ dipolar couplings will prove to be very useful in structural studies of isotopically enriched proteins and nucleic acids.[34]

Acknowledgment. We thank Frank Delaglio for developing software, Rolf Tschudin for technical support, John Kuszewski, Attila Szabo, Dennis Torchia, and Andy Wang for useful discussions, Larry Werbelow for a preprint of ref 5, and James Ferretti (National Heart, Lung and Blood Institute) for use of the AMX-360 spectrometer. Experiments at 750 MHz were carried out at the National NMR Facility at Madison, supported by grant RR02301. This work was supported by the Intramural AIDS Targeted Anti-Viral Program of the Office of the Director of the National Institutes of Health.

Supporting Information Available: One table containing the J_{NH} splittings measured at 360, 500, 600, and 750 MHz ^1H frequency from ^{15}N doublet splittings and J_{NH} splittings measured at 360, 500, and 600 MHz using fitting of the *J*-modulation pattern and one table containing the dynamic frequency shift and dipolar contributions to $^1J_{NH}$ calculated on the basis of the individual order parameters of the amide N−H bond vectors in ubiquitin and their orientation relative to the axially symmetric rotational diffusion tensor (4 pages). See any current masthead for ordering information.

JA960106N

(34) Kung, H. S.; Wang, K. Y.; Goljer, I.; Bolton, P. H. *J. Magn. Reson. Ser. B* **1995**, *109*, 323−325.
(35) Piotto, M.; Saudek, V.; Sklenar, V. *J. Biomol. NMR* **1992**, *2*, 661−665.
(36) Zhu, G.; Torchia, D. A.; Bax, A. *J. Magn. Reson. Ser. A* **1993**, *105*, 219−222.